Annals of Biomedical Engineering, Vol. 49, No. 1, January 2021 *(© 2020)* pp. 262–275
https://doi.org/10.1007/s10439-020-02536-7

Original Article

Ultra-High-Frame-Rate Ultrasound Monitoring of Muscle Contractility Changes Due to Neuromuscular Electrical Stimulation

ZHIYU SHENG,[1] NITIN SHARMA,[1,2,3,4] and KANG KIM[1,2,5,6]

[1]Department of Mechanical Engineering and Materials Science, University of Pittsburgh School of Engineering, Pittsburgh, PA 15261, USA; [2]Department of Bioengineering, University of Pittsburgh School of Engineering, Pittsburgh, PA 15261, USA; [3]Joint Department of Biomedical Engineering, North Carolina State University, Raleigh, NC 27606, USA; [4]Clinical and Translational Science Institute, University of Pittsburgh, Pittsburgh, PA 15261, USA; [5]Center for Ultrasound Molecular Imaging and Therapeutics, Department of Medicine and Heart and Vascular Institute, University of Pittsburgh School of Medicine and University of Pittsburgh Medical Center, Pittsburgh, PA 15261, USA; and [6]McGowan Institute for Regenerative Medicine, University of Pittsburgh and University of Pittsburgh Medical Center, Pittsburgh, PA 15219, USA

(Received 20 December 2019; accepted 14 May 2020; published online 1 June 2020)

Associate Editor Agata A. Exner oversaw the review of this article.

Abstract—The quick onset of muscle fatigue is a critical issue when applying neuromuscular electrical stimulation (NMES) to generate muscle contractions for functional limb movements, which were lost/impaired due to a neurological disorder or an injury. For *in situ* assessment of the effect of NMES-induced muscle fatigue, a novel noninvasive sensor modality that can quantify the degraded contractility of a targeted muscle is required. In this study, instantaneous strain maps of a contracting muscle were derived from ultra-high-frame-rate (2 kHz) ultrasound images to quantify the contractility. A correlation between strain maps and isometric contraction force values was investigated. When the muscle reached its maximum contraction, the maximum and the mean values of the strain map were correlated with the force values and were further used to stage the contractility change. During the muscle activation period, a novel methodology based on the principal component regression (PCR) was proposed to explore the strain–force correlation. The quadriceps muscle of 3 able-bodied human participants was investigated during NMES-elicited isometric knee extension experiments. Strong to very strong correlation results were obtained and indicate that the proposed measurements from ultrasound images are promising to quantify the muscle contractility changes during NMES.

Address correspondence to Nitin Sharma, Joint Department of Biomedical Engineering, North Carolina State University, Raleigh, NC 27606, USA. Electronic mail: nsharm23@ncsu.eduKang Kim, Center for Ultrasound Molecular Imaging and Therapeutics, Department of Medicine and Heart and Vascular Institute, University of Pittsburgh School of Medicine and University of Pittsburgh Medical Center, Pittsburgh, PA 15261, USA. Electronic mail: kangkim@upmc.edu

Keywords—Ultrasound imaging, Ultrasound speckle tracking, Neuromuscular electrical stimulation (NMES), Muscle fatigue effects.

INTRODUCTION

Neurological injuries such as spinal cord injury (SCI) and stroke result in mobility disabilities.[2] The resulting loss of limb functions due to paralyzed or paretic muscles impairs standing, walking, and grasping activities. To enhance or restore these limb functions, neuromuscular electrical stimulation (NMES) is used to artificially recruit extant muscle motor units (MU) *via* external electrical pulses.[31] NMES also provides therapeutic effects such as motor relearning, cardiovascular conditioning, and treatment of muscle atrophy.[31] However, compared to unimpaired volitional muscle contractions, NMES causes a rapid onset of muscle fatigue. The early fatigue onset is attributed to a non-physiological MU recruitment pattern.[6] The effectiveness of NMES is, therefore, quickly deteriorated over the time course of operation. Excessively stimulating a fatigued muscle may also cause injuries or functional task failures, which may result in secondary injuries.

To alleviate any adverse effects of muscle fatigue, improved NMES protocols[12,19,30] need to be designed. To achieve this, an effective strategy for measuring the fatigue effect is an important precursor. Recently, ultrasound imaging has been proposed as a sensory

modality to assess the changes in mechanical responses that are hypothesized to be one of the fatigue effects when a skeletal muscle performs repeated contractions. Witte *et al.* compared elastic and viscoelastic-like modifications from the ultrasound strain imaging before and after a volitional fatigue exercise of the 3rd flexor digitorum superficialis muscle.[40] The exercise-induced fatigue in the right biceps brachii muscle was investigated by a defined thickness change that was derived from the cross-sectional ultrasound images.[33] Ultrasound shear wave elastography (SWE) was used to assess muscle stiffness property and was further considered as an index to monitor muscle functions.[4,5,7,8] Siracusa *et al.* proposed SWE to assess peripheral fatigue by investigating the time course of the shear elastic modulus change of the vastus lateralis at rest.[35] Compared to other sensory modalities for measuring fatigue effects such as electromyography (EMG) or surface electromyography (sEMG),[9,10,15,21,25,28,29] mechanomyography (MMG),[18,34,41] near-infrared spectroscopy (NIRS)[36,41] and phosphorus nuclear magnetic resonance (NMR),[11] ultrasound imaging is advantageous in multiple aspects. For example, it has a relatively wide range of the field of view (FOV) in-depth and has an *in vivo* capability of collecting 2-dimensional (2D) information of a targeted muscle. Unlike signals from EMG or sEMG, signals from ultrasound images are less likely interfered by the NMES and do not have a cross-talk among neighboring muscles.

Our recent study[32] proposed the axial strain derived from ultrasound images as a promising indicator for detecting the contractility change in the human quadriceps muscle. In the study, degraded contractility referred to a decrease in the contractile deformation after applying an 80-second-long constant NMES pulse train. However, an *in vivo* continuous variation of the muscle contractility at different stages over the time course of the stimulation protocol has never been studied. The correlation between the degraded contractility and the varying force produced by a repeatedly stimulated muscle is also unknown.

Therefore, this paper aims to develop a strain imaging technology that applies an ultra-high frame rate (2 kHz) and quantifies the extremely fast muscle deformations during each NMES-elicited contraction. The quantified muscle contractility was shown to stage the NMES-induced fatigue effect by investigating the correlation between the force and the image-derived strain map. When a muscle was fully activated, the maximum and the mean of the processed strain map were correlated with the maximum force of that contraction. The strain–force correlation was further improved by using a principal component regression (PCR) based methodology when multiple strain–force measurements were taken at the high sampling rate during the muscle activation period.

FIGURE 1. (a) The experiment set-up. Programmed NMES pulse trains are sent from a stimulator through two large electrode pads attached on the thigh to elicit isometric knee extensions. The proximal electrode is placed closer to the lateral side and the distal one is placed slightly to the medial side from the midline to reach the motor points. A load cell is used to connect the shank to the leg extension machine, of which the rotary axis is rigidly fixed, and to register the force produced during isometric muscle contractions. A linear ultrasound transducer is placed in the longitudinal direction on the thigh and firmly fixed by a customized probe holder after being adjusted (as shown by the yellow arrows) to obtain the best imaging plane. (b) The fatigue protocol. To continuously stimulate the quadriceps muscle, the NMES pules trains (with each single pulse set as the amplitude of 28 mA, the pulse frequency of 35 Hz and the pulse width of 300 μs) are on for 1.5 s every 2 s (75 % duty cycle). Meanwhile, force measurements are recorded at 1kHz, and the ultra-fast ultrasound planewave imaging of 2 kHz FPS, is used to image 1 complete muscle contraction every 4 contractions. (c) Ultrasound image process. Each ultrasound image frame is reconstructed by demodulating the IQ data after the RF data is beamformed *via* a DAS beamformer. A contraction rate adaptive ultrasound speckle tracking is then performed on the selected frames of the reconstructed images to estimate the frame to frame displacement. The instantaneous displacement field of the current frame with respect to the initial reference frame, is obtained by accumulating all the frame-to-frame displacement during the past. The instantaneous strain map is obtained by taking gradient along the axial direction through an S–G filter.

To demonstrate the proposed technology, isometric knee extension experiments were performed on 3 able-bodied human participants by stimulating their quadriceps muscle under a standard NMES fatigue protocol. Ultra-high-frame-rate ultrasound images, targeted at the quadriceps muscle, were collected and synchronized with the force measurements that were registered by a load cell. A contraction-rate-adaptive ultrasound speckle tracking[23,32] was applied on the ultrasound image sequence to derive the axial strain map. The subsequent data analysis was performed to obtain and explain the strain–force correlations over the time course of the NMES protocol.

MATERIALS AND METHODS

All the procedures and protocols of the experiments were approved by the Institutional Review Board (IRB) of the University of Pittsburgh. 2 male and 1 female able-bodied human participants (of 22 to 27 years old); namely, P1, P2 and P3, joined in the experiments. Informed consent was obtained from all subjects before their participation.

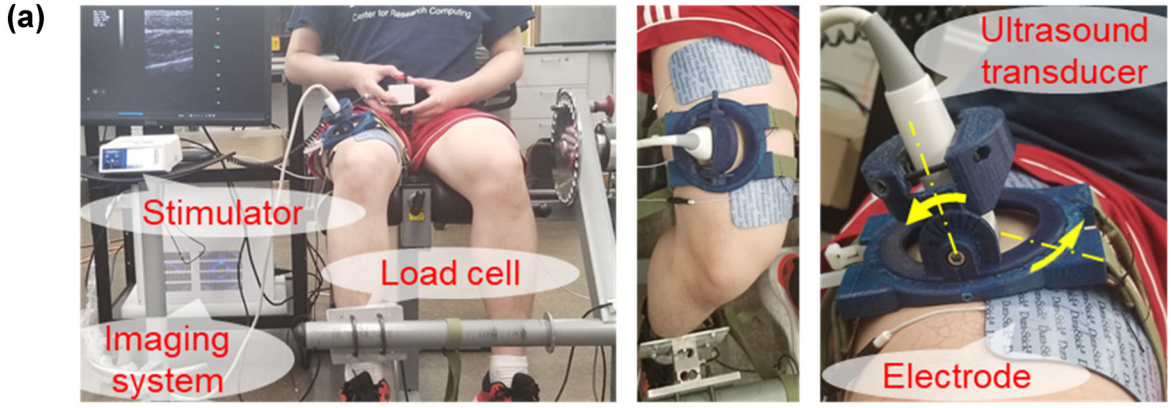
(a)
Stimulator
Load cell
Imaging system
Ultrasound transducer
Electrode

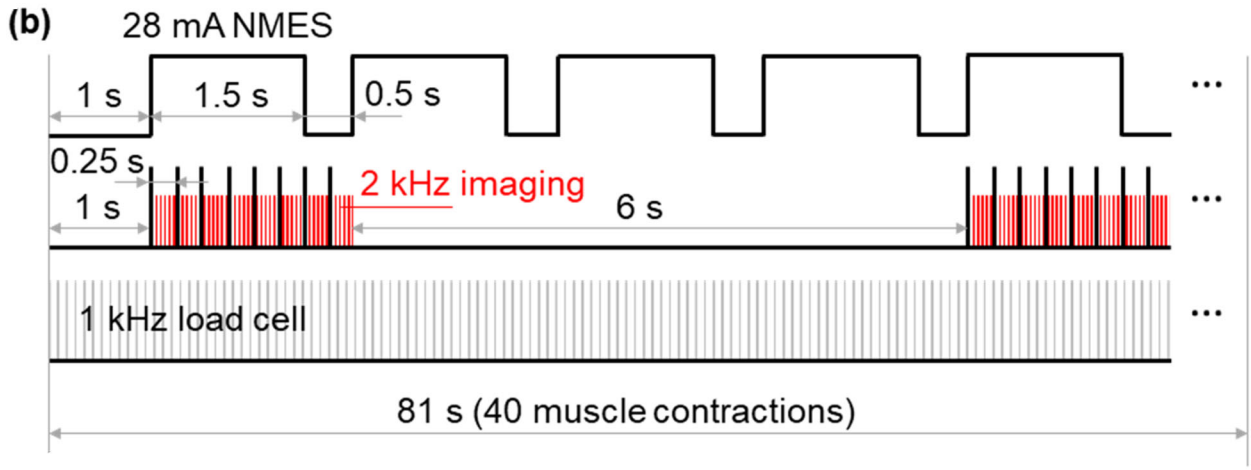
(b)
28 mA NMES
1 s
1.5 s
0.5 s
0.25 s
1 s
2 kHz imaging
6 s
1 kHz load cell
81 s (40 muscle contractions)

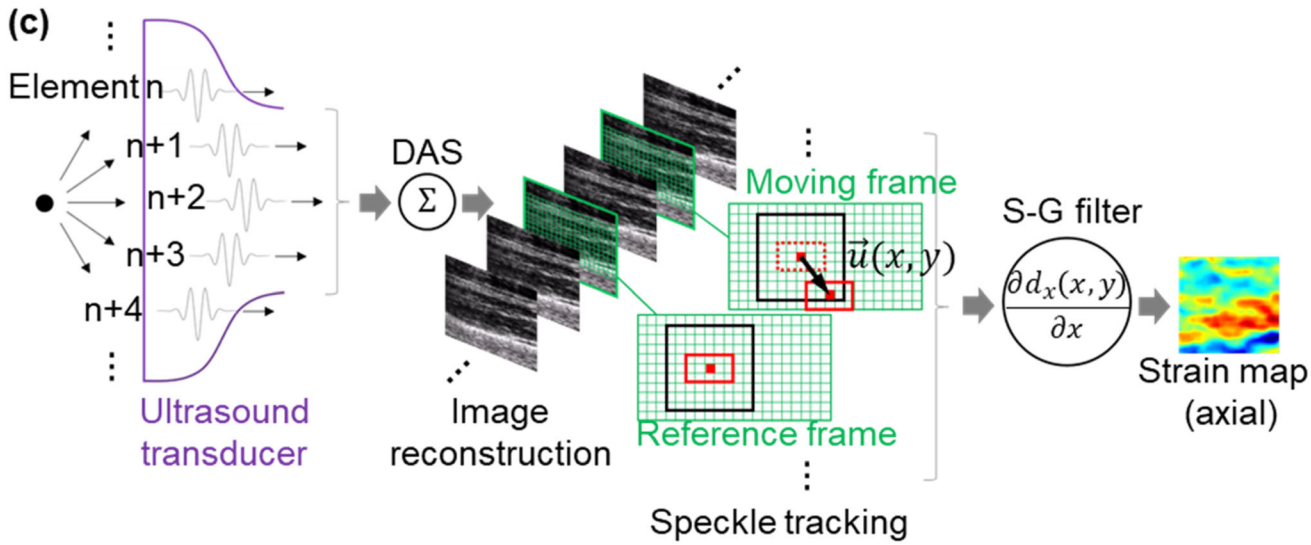
(c)
Element n
n+1
n+2
n+3
n+4
Ultrasound transducer
DAS
Σ
Image reconstruction
Moving frame
Reference frame
Speckle tracking
S-G filter
Strain map (axial)

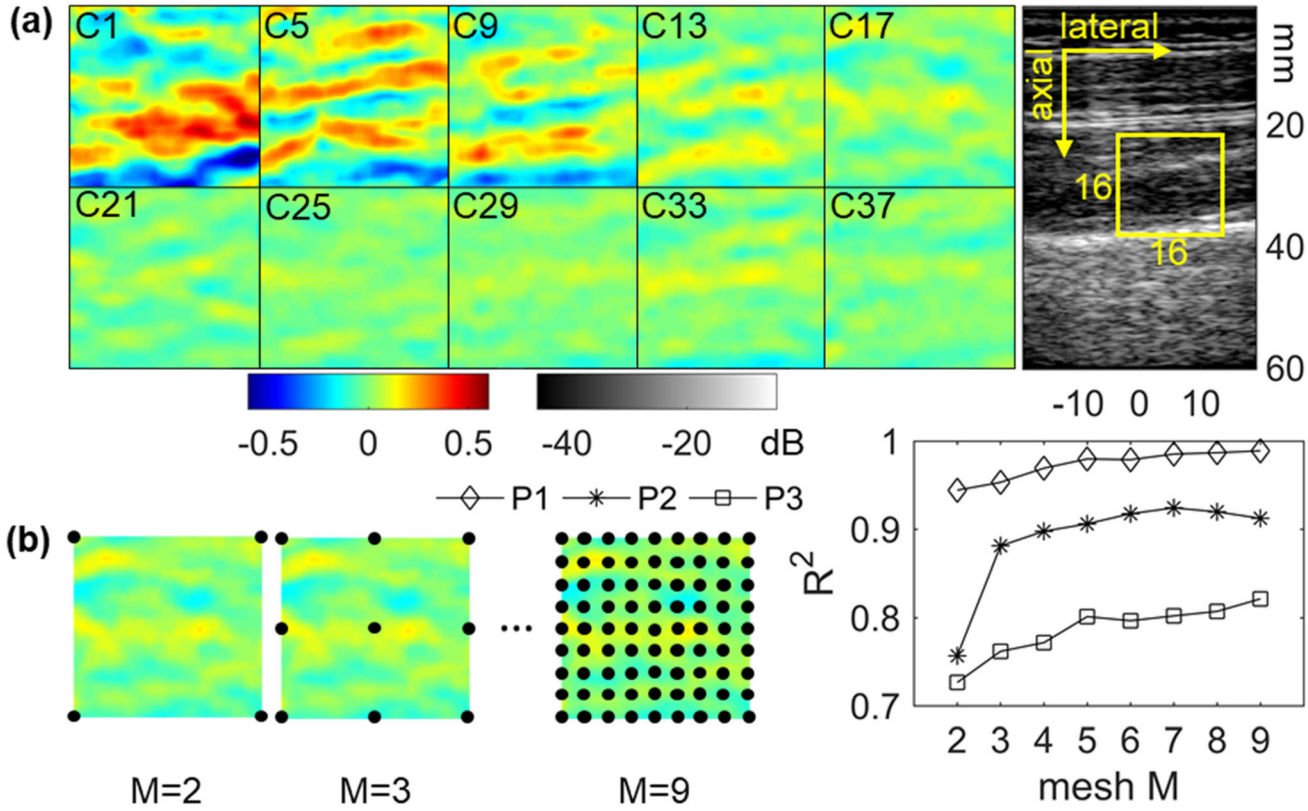

FIGURE 2. (a) The accumulated axial strain maps that are synchronized with the maximum force measured in the 1st, 5th, …, 37th muscle contractions of the human participant P1. The images were processed in a 16 mm by 16 mm ROI of the stimulated quadriceps muscle. The positive (red) strain indicates an extension while the negative (blue) strain indicates a compression along the axial direction. Each of the strain maps quantifies the accumulated deformation of the fully activated muscle with respect to the initial relaxed status. (b) A pre-defined rectangular mesh, M, used for the 2D bilinear interpolation to determine the $k_M(x, y)$ in the PCR. Goodness of fitting (R^2) can be affected by different meshes.

Experiment Set-Up

Figure 1a shows the experiment set-up. Each human participant was seated on a lab-built leg extension machine while the quadriceps muscle of the right leg was stimulated by programmed NMES pulse trains to perform isometric knee extensions. The pulse trains were sent from a commercial stimulator (Rehastim 1, HASOMED GmbH, Germany) through two electrodes (Dura-Stick Plus, 6.98 cm by 12.70 cm, Chattanooga, DJO, USA) placed on the thigh. To reach the motor points[16] of the quadriceps muscle, the proximal electrode was placed closer to the lateral side, and the distal one was placed slightly to the medial side from the midline. A load cell (LC101-150, OMEGA Engineering, USA) was attached normally to the front of the shank. The registered force readings were sampled at 1 kHz to represent the force produced by the muscle contractions, provided a constant moment arm from the knee joint to the surface of the load cell. A clinical ultrasound linear transducer (L7.5SC Prodigy Probe, S-Sharp, Taiwan) was placed in the longitudinal direction on the thigh and fixed by a customized probe holder to image the targeted quadriceps muscle. The ultrasound imaging plane was adjusted to visualize the most noticeable quadriceps muscle deformation as a response to the NMES and minimize out-of-plane motions at the same time. As a result, on a typical ultrasound image, as shown in Fig. 2a, the lateral direction (y-axis) is roughly aligned with the longitudinal fiber direction toward the distal side of the torso while the axial direction (x-axis) is orthogonal to the y-axis and points toward a deeper position beneath the skin. The ultra-fast planewave imaging, with 2 kHz frame per second (FPS), 5 MHz of center frequency and 20 MHz of sampling frequency, was implemented in the ultrasound imaging system (Prodigy, S-Sharp, Taiwan). Data synchronization among the NMES pulses, the load cell measurements, and the ultrasound image frames were configured in a Matlab/Simulink (MathWorks, USA) environment on a real-time target (QPIDe, Quanser, Canada).

Fatigue Protocol

The objective of the experiments is to investigate the strain–force correlation when a constant NMES input applies on each human participant to elicit muscle contractions and produce the effect of muscle fatigue. Since the cross-subject analysis is not the immediate focus of the current study, we used a constant stimulation set-up among all the human participants without considering the variations of their responses to the NMES. The NMES pulses were set as 28 mA of amplitude, 35 Hz of pulse frequency, and 300 μs of pulse width. These parameters were selected within a typical range of experiments on lower-limb neuroprosthetic devices that can produce predictable knee extension forces.[20] To continuously stimulate the quadriceps muscle, as illustrated by Fig. 1b, the pulse trains were on for 1.5 s every 2 s (75 % duty cycle). The 0.5 s rest period lets muscle recover to the relaxed geometry between consecutive contractions. As a result, after the system initialization of 1 s, in total, 40 muscle contractions were performed during an 80-second-long period. A sequence of ultrasound image frames was collected to include 1 complete muscle contraction every 4 contractions.

Image Process

During each of the 10 imaged muscle contractions, image frames, from the time instant when the first NMES pulse occurred to the time instant when the maximum force was reached, were extracted for analysis. Fig. 1c illustrates the image processing procedure. Each image was reconstructed by demodulating the in-phase and quadrature (IQ) data after beamforming the raw ultrasound radio frequency (RF) data *via* a delay-and-sum (DAS) beamformer. A contraction rate adaptive ultrasound speckle tracking[23,32] was performed on the selected frames of the reconstructed images to estimate the 2D frame-to-frame displacement. The frames were selected based on the observed rate of the muscle contractions. When muscle moves very fast, tracking is applied between every two consecutive frames. This ensures the quasi-static tracking and minimizes the speckle decorrelation. When muscle contracts at a relatively low speed, tracking is performed only between selected frames from the image sequence, by comparing which, a discernable motion can be visualized. The rest of the frames were all skipped. This criterion helps reduce unnecessary noise accumulation when summing the frame to frame tracking results. An instantaneous displacement field, $d(x,y) = \left(d_x(x,y), d_y(x,y)\right)$, of each tracked image frame, with respect to an initial reference frame, was then obtained by accumulating all the tracked frame-to-frame displacement during the past. The instantaneous displacement fields of the skipped frames were calculated by interpolation. According to the assumptions in our previous study,[32] the axial strain map, $s_{ax}(x,y)$, defined based on the principal stretches, was then derived at each position, (x, y), by calculating the spatial derivative of $d_x(x, y)$, as $s_{ax}(x,y) = \partial d_x(x,y)/\partial x$. A Savitzky–Golay (S–G) filter with the kernel length in a range from 3.0 to 3.5 mm was implemented to differentiate $d_x(x, y)$.

Data Analysis

During each experiment under the designed protocol, 40 NMES-elicited muscle contractions were performed in 80 s. In each of the contractions, the maximum force was reached and recorded after a transient muscle activation period. According to Riener *et al.*[27] where they modeled the fatigue effect using first order dynamics, the maximum force produced by the fully activated muscle during each contraction should decay almost exponentially under a constant NMES input. Therefore, an exponential model, $y = \alpha_1 e^{\alpha_2 x} + \alpha_3$, was fitted between the maximum force data and the index number of muscle contractions ($x = 1, 2, \ldots, 40$) by using the Levenberg–Marquardt nonlinear least squares algorithm.[22,24,26] The constants, α_1 and α_3, reflect the initial maximum force and the minimum force that is attained when the muscle is completely fatigued. α_2 reflects the fatigue constant, i.e., the rate of decay, which is expected to be a negative number. The frame of the processed axial strain map, which was synchronized to the maximum force during a contraction, was selected to calculate the mean and the maximum. By considering the local extension of the target muscle in the FOV as the major signal that quantifies the contractile deformation, a thresholding procedure that sets the negative values on the map to be zero was applied. The reason for thresholding rather than excluding the negative values is in order not to bias the calculation of the area fraction of the positive axial strains with respect to the total strain map when calculating the mean. Simple linear regressions ($n = 10$) were performed between the maximum force and the strain mean, as well as between the maximum force and the maximum strain. A t test was performed on each of the nonlinear and linear regression coefficients, which was compared to zero with the critical p value chosen as 0.05.

To further investigate the correlation between the strain map and the force during the transient muscle activation period, PCR was used to fit the model as,

$$F = b_{0,M} + \sum_y \sum_x k_M(x,y) s(x,y) \Delta, \qquad (1)$$

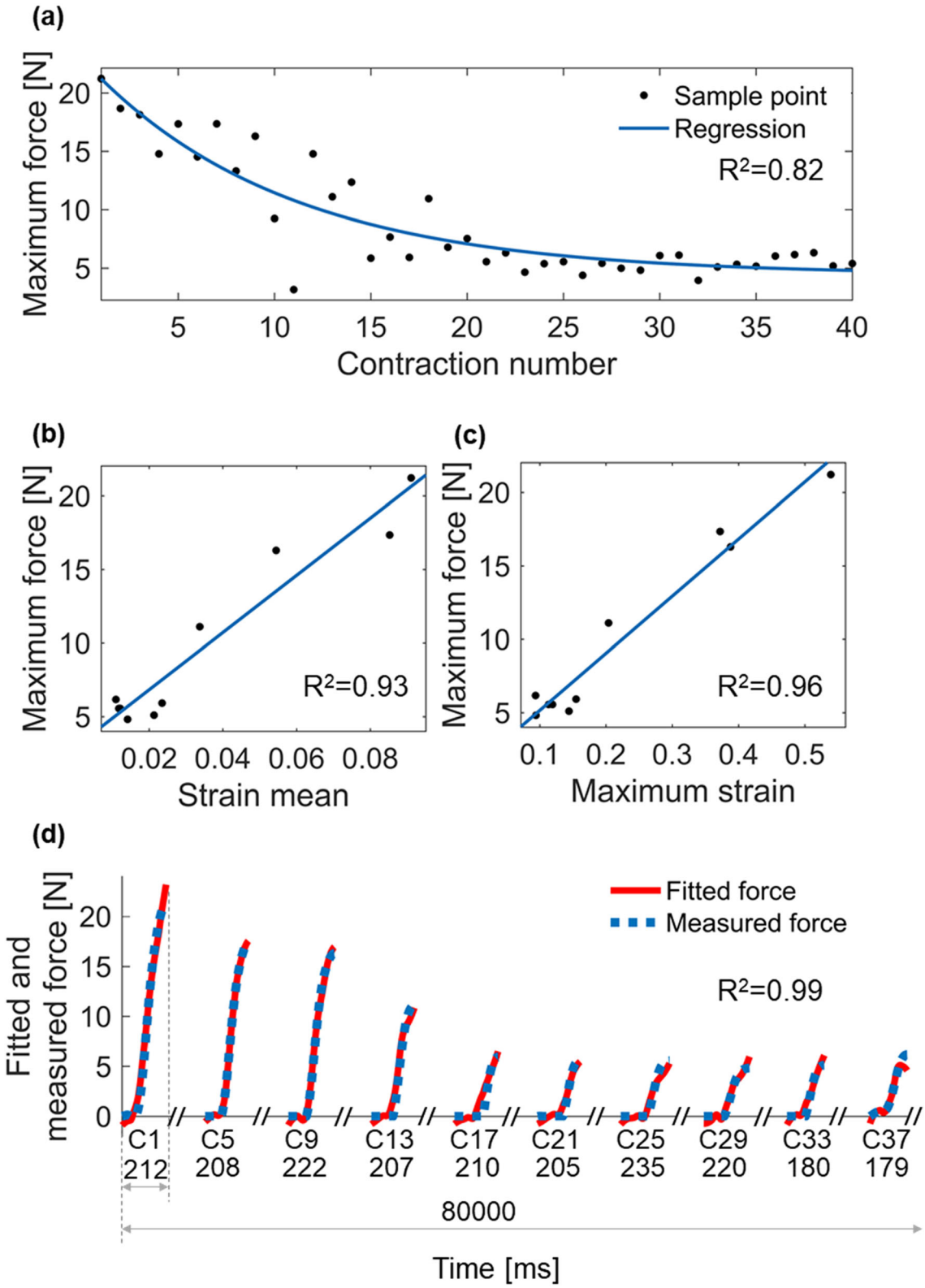
(a)
Maximum force [N]
Contraction number
Sample point
Regression
R²=0.82
(b)
Maximum force [N]
Strain mean
R²=0.93
(c)
Maximum force [N]
Maximum strain
R²=0.96
(d)
Fitted and measured force [N]
Fitted force
Measured force
R²=0.99
C1 212
C5 208
C9 222
C13 207
C17 210
C21 205
C25 235
C29 220
C33 180
C37 179
80000
Time [ms]

◀**FIGURE 3. Data analysis of human participant P1. (a) The maximum force fitted to an exponential curve shows a decreasing trend and validate the effectiveness of the fatigue protocol. (b) Under the fatigue protocol, the decreased maximum force during each contraction correlates with the decreased mean value of the synchronized strain map. (c) The decreased maximum force during each contraction correlates with the decreased maximum value of the synchronized strain map. (d) The measured force (blue dashed lines) and the fitted force (solid red lines) using the processed strain images *via* the proposed PCR-based methodology. The results include the transient period during each contraction when the muscle contracts from the relaxed status to the fully activated status. The time axis records the duration of each contraction. The breaks in the axis indicate an omitted time period for presentation purposes. Details of the fitting results in (a)–(d) can be found in Tables 1 and 2.**

where the response variable, F, is the instantaneous force produced by the stimulated muscle contraction. $s(x, y)$, after thresholding the negative values to be zero, is the positive axial strain of a pixel at a position of (x, y) mm from the image frame that is synchronized with F. In Eq. (1), (mm^2/pixel) is the area of a single pixel, $b_{0,\mathrm{M}}$ is the intercept and $k_{\mathrm{M}}(x, y)$ is the unknown spatially dependent function. $b_{0,\mathrm{M}}$ and $k_{\mathrm{M}}(x, y)$ need to be identified *via* the regression. In this study, a 2-dimensional (2D) bilinear interpolation was used to estimate the $k_{\mathrm{M}}(x, y)$ based on a pre-defined rectangular mesh, M, as illustrated in Fig. 2b. The values of the interpolant at the mesh grids are the regression coefficients of the multi-variate linear regression that adopts PCR. For each human participant, a total of 40 muscle contractions was divided into 3 groups according to the maximum axial strain of each contraction that was normalized to the overall maximum, $s_{\max}$, among all the 40 contractions. A muscle contraction, of which the normalized maximum axial strain falls in the ranges of [70.0, 100] %, [40.0, 70.0] % and [0, 40.0] %, respectively, belongs to the group, G1, G2 and G3, respectively. In each group, the PCR regression was performed to identify $b_{0,\mathrm{M}}$ and $k_{\mathrm{M}}(x, y)$ of this group. Figs. 3d, 4d, and 5d of P1, P2, and P3, respectively, show the fitting results during all the activation periods of the stimulated muscle contractions. The presented results of P1, P2, and P3, respectively, are based on a mesh $M = 9$, $M = 7$, $M = 7$, respectively. The dashed blue lines refer to the force measurement from the experiments while the solid red line depicts the force calculated from Eq. (1) by using the fitted parameters, $b_{0,\mathrm{M}}$ and $k_{\mathrm{M}}(x, y)$. The p value of the intercept was calculated using an F test by comparing the derived intercept with 0. The p value of a specific regression coefficient, associated with a principal component (PC), was calculated by an F test that compared the fitted model using all the PCs with the fitted model using the remaining PCs after excluding that specific PC. Any principal component with $p > 0.05$ was considered non-significant and was excluded from the regression process. Details of the implementation of the PCR can be found in the supplementary information.

RESULTS

Validation of the Fatigue Protocol

For each human participant (P1, P2, and P3), the exponential curve, $y = \alpha_1 e^{\alpha_2 x} + \alpha_3$, was fitted between the maximum force data and the number of muscle contractions. The results were shown in Figs. 3a, 4a, and 5a, respectively, as $R^2 = 0.82$, $R^2 = 0.95$ and $R^2 = 0.98$, respectively. More details of the fitting results are provided in Table 1. Because a reduction in the maximum force is commonly noted as a fatigue indicator,[38] the significant negative values of α_2 ($p < 0.05$) validates the effectiveness of the applied fatigue protocol of each human participant.

Quantification of the Muscle Contractility Via the Axial Strain Map

The accumulated axial strain maps, $s(x,y)$ were processed from ultrasound images (See the method section for a detailed description.) in a 16 mm by 16 mm region of interest (ROI) of the stimulated quadriceps muscle. Supplementary Videos S1, S2, …, S10 online show the processed results during each of the ith muscle contraction, C_i ($i = 1, 5, 9, \ldots, 37$), over the time course of the fatigue protocol. Fig. 2a presents the frames of the strain maps that are synchronized with the maximum force measured in each contraction. Therefore, these strain maps quantify the accumulated deformation of the fully activated muscle with respect to the initial relaxed status. At a local position, the positive (red) strain indicates an extension, while the negative (blue) strain indicates a compression along the axial direction of the ultrasound beam. As it can be observed from the strain maps of the 1st and 5th contractions, C1 and C5, relatively large positive strain areas are initially distributed inside the ROI. There are also negative strain values mainly located at a deeper axial position ($x > 35$ mm), which is the boundary of the vastus intermedius (VI) and closer to the femur. In subsequent contractions, both the positive and negative axial strain gradually decrease, as shown by C9, C13, and C17. The strain maps become almost uniform zero after C21. This implies that even though the same NMES input is maintained, there is no longer a noticeable muscle contraction detected by ultrasound

TABLE 1. Nonlinear and linear regression results of each human participant.

	Decay of max. force ($y = \alpha_1 e^{\alpha_2 x} + \alpha_3$)					Max. force and strain mean ($y = \alpha_1 x + \alpha_2$)				Max. force and max. strain ($y = \alpha_1 x + \alpha_2$)			
	α_1 (p value)	α_2 (p value)	α_3 (p value)	R^2	n	α_1 (p value)	α_2 (p value)	R^2	n	α_1 (p value)	α_2 (p value)	R^2	n
P1	19 (1.4e−14)	− 0.097 (2.1e−5)	4.4 (1.8e−5)	0.82	40	19e1 (0.0093)	2.9 (6.6e−6)	0.93	10	39 (7.7e−7)	1.3 (0.1)	0.96	10
P2	37 (4.8e−37)	− 0.030 (6.5e−26)	0	0.95	40	65 (0.0051)	14 (0.00081)	0.65	10	17 (0.0035)	12 (0.0041)	0.66	10
P3	12e1 (4.3e−40)	− 0.041 (1.2e−31)	0	0.98	40	33e1 (3.3e−6)	16 (0.011)	0.94	10	90 (8.8e−6)	1.8 (0.79)	0.93	10

The decay of the maximum force during each contraction was fitted to an exponential curve, $y = \alpha_1 e^{\alpha_2 x} + \alpha_3$. A significant negative α_2 indicates the effectiveness of the fatigue protocol applied on each participant. The maximum force during each contraction was correlated with the mean and maximum value, respectively, of the synchronized axial strain map. α_1 and α_2 in $y = \alpha_1 x + \alpha_2$ were identified by a linear regression. All the p values were calculated by t tests with the critical value chosen as 0.05.

TABLE 2. The goodness of fitting of using Eq. (1) to explain the force–strain correlation during the transient muscle activation period.

	P1			P2			P3		
Contr. #Contr. #	G1 C1, C3	G2 C2	G3 C4–C10	G1 C1, C2	G2 C3, C4	G3 C5–C10	G1 C1–C3	G2 C4–C6	G3 C7–C10
n	436	209	1443	533	602	1814	693	898	1269
Group R^2	0.99	1.0	0.95	0.98	0.97	0.80	0.70	0.96	0.81
Intercept (p value)	− 0.81 (2.1e−70)	− 0.49 (3.6e−64)	− 0.71 (8.9e−271)	− 1.0 (5.6e−40)	− 1.25 (1.8e−57)	0.47 (2.0e−12)	− 16 (1.6e−79)	− 3.5 (1.0e−97)	3.0 (2.1e−98)
Eig. %	100	99.9	99.7	100	100	97.7	99.9	99.8	74.4
Overall R^2	0.99			0.92			0.80		

The fitting was calculated by a linear PCR that was applied on each human participant in each data group (see the text for descriptions). Contr. # represents the index of the muscle contraction over the time course during the fatigue protocol. The PCR only keeps significant PCs ($p \leq 0.05$) while removing the non-significant ones ($p > 0.05$) that are determined by F tests. Eig. % represents the sum of the eigenvalues, which corresponds to the significant PCs, of the covariance matrix.

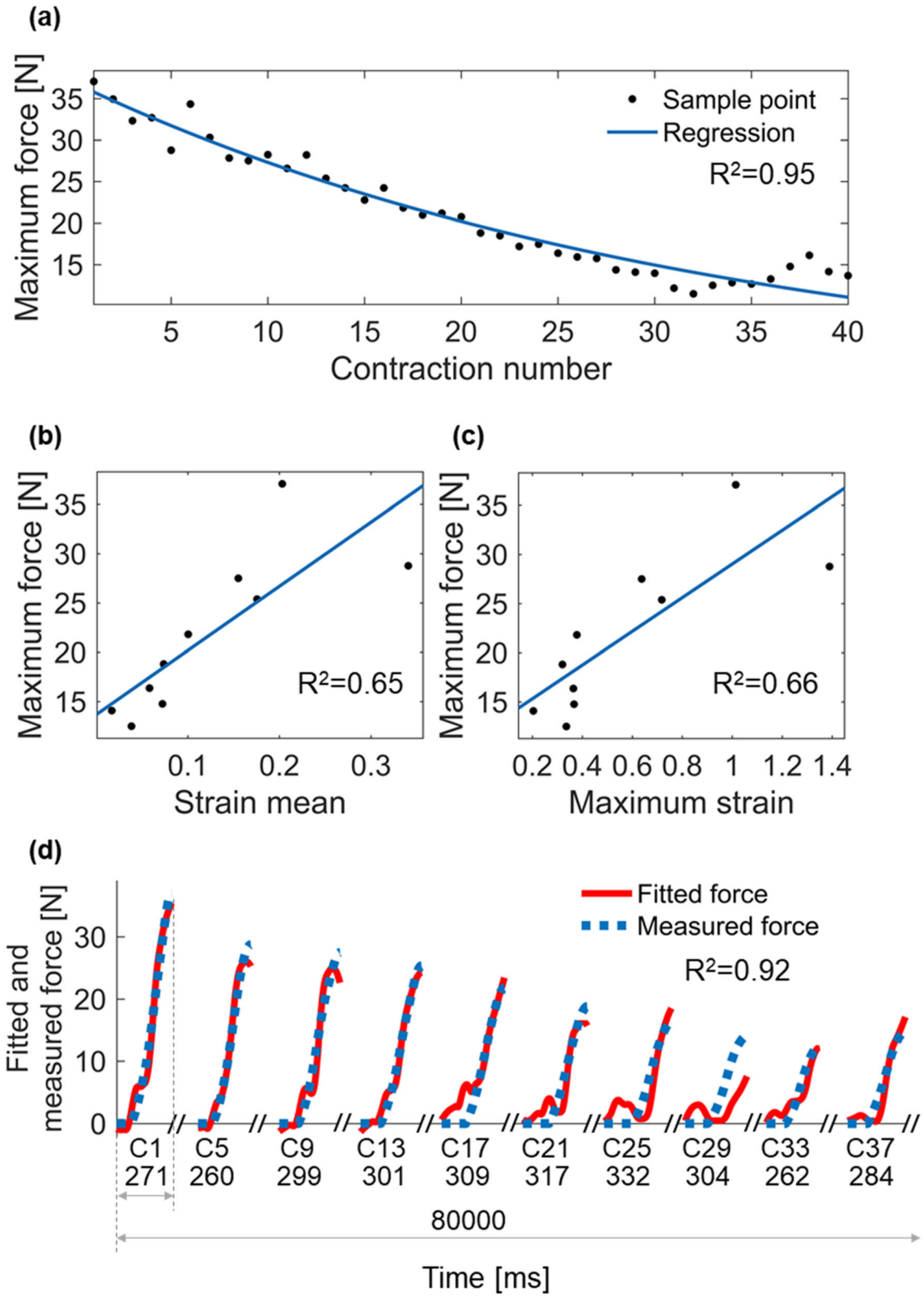

FIGURE 4. Data analysis of human participant P2.

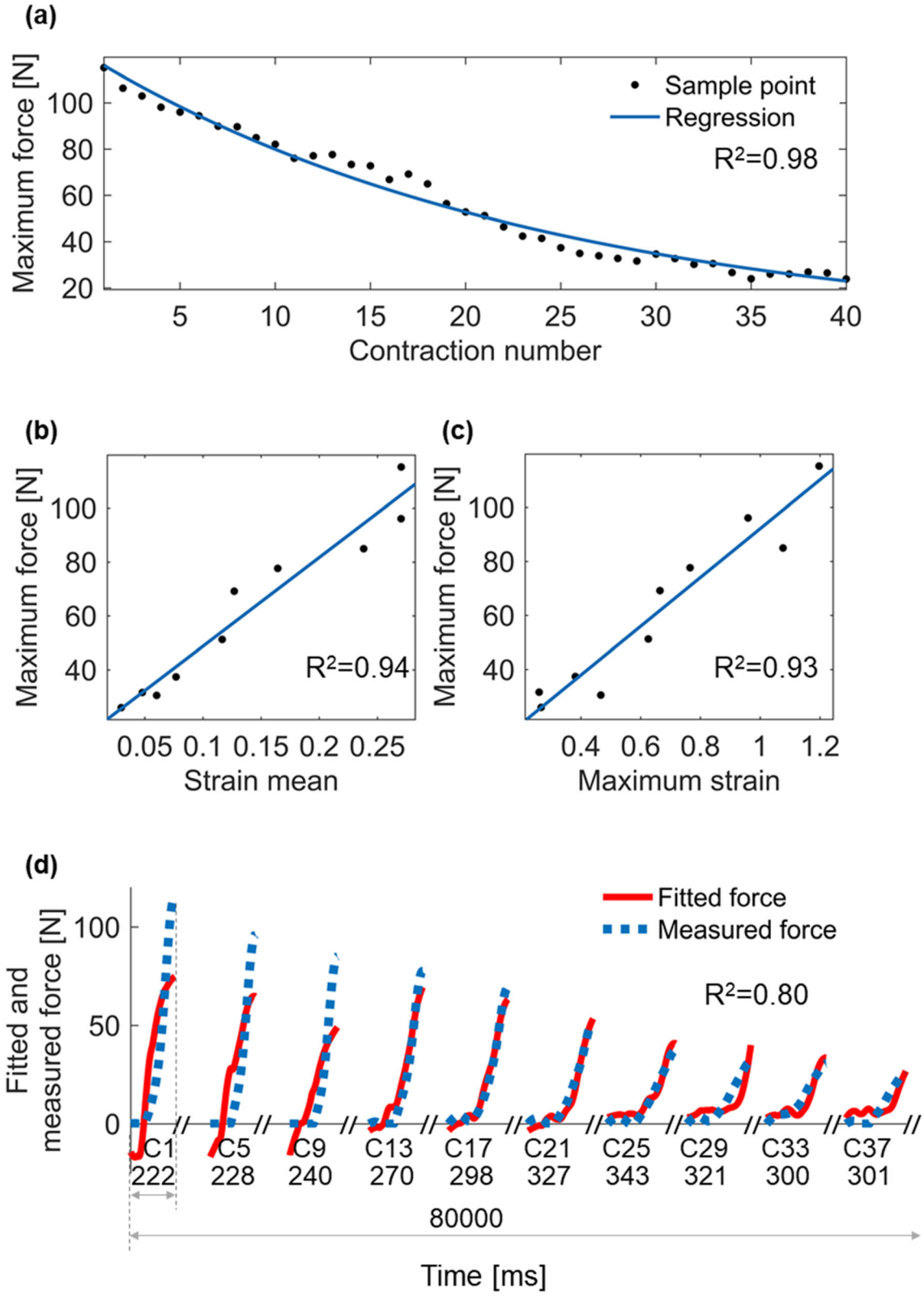

FIGURE 5. Data analysis of human participant P3.

images inside the chosen ROI. This observation is consistent with the force measurement that is below 30 % of the initial level and indicates an overall degraded muscle contractility. The observations are consistent among the participants.

Correlation Between the Axial Strain and the Maximum Force

To quantitatively stage the muscle contractility change *via* the axial strain map, the mean and the maximum value of the positive axial strain were investigated. After thresholding all the negative $s(x, y)$ to be zero, linear regressions between the maximum force and the mean of the strain map was performed, as shown by Figs. 3b, 4b and 5b of human participants P1, P2 and P3, respectively. Fitting results; i.e., $R^2 = 0.93$, $R^2 = 0.65$ and $R^2 = 0.89$ were obtained for P1, P2 and P3, respectively. The results indicate a strong to very strong correlation. Figs. 3c, 4c and 5c of P1, P2 and P3, respectively, shows the linear regression results between the maximum force and the maximum of the strain map. The goodness of fitting, that is, $R^2 = 0.96$, $R^2 = 0.66$, and $R^2 = 0.93$ of P1, P2 and P3, respectively, indicates a strong to very strong correlation. Details of the fitting results are provided by Table 1.

Correlation Between the Axial Strain and the Force Response to NMES During the Transient Period

During the transient period when the muscle contracts from a relaxed position to its maximum capacity, multiple strain–force measurements are available due to a very high sampling rate (2 kHz). Therefore, an improved strain–force correlation result can be achieved by fitting Eq. (1) using PCR. Figs. 3d, 4d and 5d of P1, P2 and P3, respectively, shows the fitting results during all the transient periods. The presented results of P1, P2 and P3, respectively, are based on a mesh $M = 9$, $M = 7$, $M = 7$, respectively. The dashed blue lines refer to the force measurement from the experiments while the solid red line depicts the force calculated from Eq. (1) by using the fitted parameters, $b_{0,\mathrm{M}}$ and $k_{\mathrm{M}}(x,y)$. The goodness of fitting is summarized in Table 2. Complete information of the PCR results can be found in the Supplementary Table S1, S2 and S3.

DISCUSSION

The positive axial strain located inside the ROI, as shown in Fig. 2, was chosen to quantify the resultant contractile deformation of the entire stimulated quadriceps muscle without precisely distinguishing the contributions from rectus femoris, vastus lateralis, vastus medialis and vastus intermedius. This is due to the fact that the local axial extensions in this ROI were observed as the most noticeable and robust signals during each muscle contraction and were also shown, in our previous study,[32] to have a significant reduction when the muscle is completely fatigued. In addition, by observing Fig. 2a, though the negative strain (local compression) also had a substation reduction during the fatigue protocol, it is more likely a passive deformation due to the interaction with the neighboring tissues. This occurred especially at locations with more constrained boundary conditions, e.g., the boundaries between different muscle layers, shallower locations close to the skin or deeper locations closer to the bone. Therefore, these areas were considered of zero strain when calculating the mean of the positive axial strain over the ROI. Consequently, Figs. 3a, 3b, 4a, 4b, 5a, 5b, and Table 1 indicate that during the validated fatigue protocol, when the contraction of the quadriceps muscle was fully activated, both the mean and maximum of the positive axial strain had a strong correlation with the maximum force. The maximum reflects the overall magnitude of the contractile deformation. The mean is calculated by a weighted sum of the strain values at every pixel location. The weight is determined by the area fraction that a particular strain value occupies with respect to the total area of the ROI. Therefore, the mean accounts for the spatial distribution of the local muscle deformation (extensions). The results suggest that the positive axial strain map can be a potential marker to monitor the degraded muscle contractility during NMES applications.

The rationale of applying Eq. (1) with the PCR to investigate the strain–force correlation during the transient muscle activation period is explained as follows. During each muscle contraction, we observed that, inside the ROI, the muscle deformation is monotonically increasing until a steady state. The observed increase in the deformation is likely an outcome of the increasingly generated internal forces in the muscle fibers that belong to activated MUs. An activated MU refers to the MU that is recruited by the NMES and incrementally releases impulsive mechanical energy from the contractile elements[39] to produce the force. It is, therefore, reasonable to use the deformation to quantify the increasing force that is contributed from the muscle during the activation period towards the maximum capacity of all the activated MUs. The maximum capacity is then affected under a long period of stimulation because, over more and more contractions under constant stimulation, MUs have a decreasing capability of delivering mechanical energy due to a combination of multiple physiological factors[3] known as the fatigue effects. As a result, the

instantaneous force response to NMES during each contraction is expected to correlate with the axial strain map that reflects the observed contractile deformation as,

$$F = a \int_A k(x,y)s(x,y)dA + b, \quad (2)$$

which is exactly same as, but a continuous version of Eq. (1). dA is a small area around a local position (x, y). $k(x, y)$ is a weight function to be applied when the strain field is integrated to estimate the overall contributions to produce the force. The spatial dependency of $k(x, y)$ provides the flexibility for considering the inhomogeneous factors, for example, the possibility that similar values of local deformation might be a result of different internal forces in different regions due to inhomogeneous tissue properties, and thus represent for different contributions to the total force produced by the contraction. This usually leads to a higher correlation than simply using the average strain because the spatial flexibility increases the degree-of-freedom of the regression model. A higher correlation is useful in this study because it better relates the change in force to the change in muscle contractility. a, which can be lumped into $k(x, y)$, and b are scale and offset factors, respectively, which accounts for the limited ROI where the strain map is processed.

The advantage of employing the PCR is that the covariates are transformed along PC axes that are uncorrelated with each other. Therefore, non-significant PCs, compared with the full model fitted using all the PCs, can be removed, and consequently, the order of the fitted model can be reduced. In addition, in this study, all the covariates are in the same unit. Therefore, before the regression procedure, removing PCs with extremely small eigenvalues of the covariance matrix (with the remaining PCs representing more than 90% of the sum of all the eigenvalues) can avoid fitting a data component with non-dominant variance, which is more likely noise from signal processing.

Performing the PCR in separate groups, G1, G2, and G3 assumes different $k(x, y)$ values in different stages of the stimulation protocol, which are reflected by the discrepancy in the maximum axial strain. Though the described concept of $k(x, y)$ is different from the elasticity in continuum mechanics, it can still be affected by varying tissue properties. For example, in a stiffer muscle, the local extensions are likely of smaller magnitude even though there is a large amount of activated MUs so that a large force is generated. To the best of our knowledge, there is no solid consensus among literature showing that tissue properties are time-invariant as muscle performs more and more contractions under NMES. In fact, results from several SWE studies[4,7,35] indicate a possible change in the shear elastic modulus. Therefore, to account for a potential change in tissue properties, an ad hoc strategy was applied to use variant values of $k(x, y)$ from group to group. Currently, the simple criterion for grouping the data is to evenly divide the overall 0–100% maximum axial strain into 3 intervals that correspond to 3 contractility stages indicated by the force-maximum strain correlation. The first interval is a little larger by considering the relatively low sensitivity of the signal processing at low strain values. More data groups are not desired because this will further reduce the sample size of the regression inside each group and will likely degrade the overall robustness of the PCR results. Future studies may introduce a time-dependent $k(x, y, t)$ to better facilitate the continuous time-variant feature. For the purpose of comparison, a time-invariant $k(x, y)$ among all the 40 muscle contractions during the fatigue protocol yields a reduced (but still strong) correlation results reported as $R^2 = 0.98$ ($n = 2088$), $R^2 = 0.83$ ($n = 2949$) and $R^2 = 0.70$ ($n = 2860$) of P1, P2 and P3, respectively, after removing all the non-significant PCs ($p > 0.05$).

For P1, P2 and P3, the values of overall R^2 obtained under either condition, (when $k(x, y)$ is assumed time invariant or when the regression is performed in separate groups), indicate strong to very strong correlations between the axial strain map and the instantaneous force. According to Table 2, there was a relatively large negative intercept in G1 of P3, and the fitted curve among those data points underestimated the force measured from the experiment, as shown by Fig. 5d. We speculate that approximating the muscle contraction outside the ROI by scaling and offsetting with a and b in Eq. (2) might not work perfectly when the contractile response to the NMES is not homogenous in the entire stimulated muscle volume. Especially when the scale of both the deformation and force were relatively large due to a strong muscle response during G1 of P3, the error caused by spatial extrapolation outside the ROI using a linear relationship with a and b was likely to increase. In future studies, this suggests a new experiment design that synchronously uses multiple ultrasound transducers to cover an extended ROI of the targeted muscle. Nonetheless, the overall quality of the correlation result was not undermined. The proposed methodology demonstrates the feasibility of using Eq. (1) to explain the degraded muscle response to NMES during the fatigue protocol.

Different choices of the mesh, M can result in slightly different fitting results of Eq. (1). As shown in Fig. 2b, an increased M overall improved the goodness of fitting (R^2). A large M does not artificially enrich the information extracted from the axial strain map. Instead, it allows more spatial flexibility of estimating

$k(x, y)$, and later the PCR will eliminate the non-significant PCs if such increased flexibility is found unnecessary by F tests. Particularly, $M = 1$ yields a constant $k(x, y)$ and is equivalent to correlate the mean of the strain map to the force response. R^2 curves in Fig. 2b provides a guideline of selecting M. Also, the choice of $M = 9$, $M = 7$ and $M = 7$ of the presented results P1, P2 and P3, respectively, was also based on the criteria that a single element enclosed by 4 grid points should be greater than 2 by 2 mm. This potentially increases the robustness of the results by reducing the sensitivity of the fitting to an occasional potential noise distributed on the strain map.

The obtained correlation results are from data analysis on each human participant. The results indicate that, during NMES applications, especially those used for generating functional movements, the ultra-high-frame-rate ultrasound imaging can be developed into a technology that continuously monitors users' muscle contractility change compared to their initial muscle capability under a certain stimulation input. Further studies, such as investigating and comparing the correlation across different subjects (of different gait abilities due to age, disease, *etc*.), tissue mechanical property assessment, and repeated experiments under different NMES protocols are required. This will lead to establishing a general strain–force model (in the form of Eq. (1)) that can describe the underlying physiology and biomechanics of the NMES-induced muscle fatigue. For the cross-subject comparison, the experiments need to be performed in an extended sample size, and the NMES parameters need to be tailored for each human participant to create a fixed portion of each one's maximum voluntary contraction. For assessing tissue mechanical properties, SWE is a potential image modality that can be implemented to the current ultrasound imaging set-up.

Overall, the experimental results in this study suggest that the proposed novel ultrasound imaging-based approach is promising to estimate the instantaneous contractile force, which is a commonly used indicator[38] to assess the effect of NMES-induced muscle fatigue. In future studies, this methodology will be implemented in real-time and applied to improve the control performance of an NMES-based neuroprosthesis[1,13,14,17,20,37] in a way that the assessed degree of contractility is used as feedback information to modulate the delivered NMES dosage.

ELECTRONIC SUPPLEMENTARY MATERIAL

The online version of this article (https://doi.org/10.1007/s10439-020-02536-7) contains supplementary material, which is available to authorized users.

ACKNOWLEDGMENTS

This research is supported by NSF award number: 1646009. Any opinions, findings and conclusions or recommendations expressed in this material are those of the authors and do not necessarily reflect the views of NSF. This research was supported in part by the University of Pittsburgh Center for Research Computing through the resources provided.

REFERENCES

[1]Alibeji, N. A., N. A. Kirsch, and N. Sharma. An adaptive low-dimensional control to compensate for actuator redundancy and FES-induced muscle fatigue in a hybrid neuroprosthesis. *Control Eng. Pr.* 59:204–219, 2017.

[2]Alibeji, N. A., V. Molazadeh, F. Moore-Clingenpeel, and N. Sharma. A muscle synergy-inspired control design to coordinate functional electrical stimulation and a powered exoskeleton: artificial generation of synergies to reduce input dimensionality. *IEEE Control Syst. Mag.* 38:35–60, 2018.

[3]Allen, D. G., G. D. Lamb, and H. Westerblad. Skeletal muscle fatigue: cellular mechanisms. *Physiol. Rev.* 88:287–332, 2008.

[4]Andonian, P., M. Viallon, C. Le Goff, C. de Bourguignon, C. Tourel, J. Morel, G. Giardini, L. Gergelé, G. P. Millet, and P. Croisille. Shear-wave elastography assessments of quadriceps stiffness changes prior to, during and after prolonged exercise: a longitudinal study during an extreme mountain ultra-marathon. *PLoS ONE* 11:e0161855, 2016.

[5]Ateş, F., F. Hug, K. Bouillard, M. Jubeau, T. Frappart, M. Couade, J. Bercoff, and A. Nordez. Muscle shear elastic modulus is linearly related to muscle torque over the entire range of isometric contraction intensity. *J. Electromyogr. Kinesiol.* 25:703–708, 2015.

[6]Bickel, C. S., C. M. Gregory, and J. C. Dean. Motor unit recruitment during neuromuscular electrical stimulation: a critical appraisal. *Eur. J. Appl. Physiol.* 111:2399–2407, 2011.

[7]Bouillard, K., M. Jubeau, A. Nordez, and F. Hug. Effect of vastus lateralis fatigue on load sharing between quadriceps femoris muscles during isometric knee extensions. *J Neurophysiol* 111:768–776, 2014.

[8]Bouillard, K., A. Nordez, and F. Hug. Estimation of Individual Muscle Force Using Elastography. *PLoS ONE* 6:e29261, 2011.

[9]Chesler, N. C., and W. K. Durfee. Surface EMG as a fatigue indicator during FES-induced isometric muscle contractions. *J. Electromyogr. Kinesiol.* 7:27–38, 1997.

[10]Cifrek, M., V. Medved, S. Tonković, and S. Ostojić. Surface EMG based muscle fatigue evaluation in biomechanics. *Clin. Biomech.* 24:327–340, 2009.

[11]Dawson, M. J., D. G. Gadian, and D. R. Wilkie. Muscular fatigue investigated by phosphorus nuclear magnetic resonance. *Nature* 274:861, 1978.

[12]Doll, B. D., N. A. Kirsch, X. Bao, B. E. Dicianno, and N. Sharma. Dynamic optimization of stimulation frequency to reduce isometric muscle fatigue using a modified Hill–Huxley model. *Muscle Nerve* 57:634–641, 2018.

[13]Downey, R. J., T. H. Cheng, M. J. Bellman, and W. E. Dixon. Switched tracking control of the lower limb during asynchronous neuromuscular electrical stimulation: theory and experiments. *IEEE Trans. Cybern.* 47:1251–1262, 2016.
[14]Farris, R. J., H. A. Quintero, and M. Goldfarb. Preliminary evaluation of a powered lower limb orthosis to aid walking in paraplegic individuals. *IEEE Trans. Neural Syst. Rehabil. Eng.* 19:652–659, 2011.
[15]Georgakis, A., L. K. Stergioulas, and G. Giakas. Fatigue analysis of the surface EMG signal in isometric constant force contractions using the averaged instantaneous frequency. *IEEE Trans. Biomed. Eng.* 50:262–265, 2003.
[16]Gobbo, M., N. A. Maffiuletti, C. Orizio, and M. A. Minetto. Muscle motor point identification is essential for optimizing neuromuscular electrical stimulation use. *J. Neuroeng. Rehabil.* 11:17, 2014.
[17]Ha, K. H., S. A. Murray, and M. Goldfarb. An approach for the cooperative control of FES with a powered exoskeleton during level walking for persons with paraplegia. *IEEE Trans. Neural Syst. Rehabil. Eng.* 24:455–466, 2016.
[18]Ibitoye, M. O., N. A. Hamzaid, J. M. Zuniga, and A. K. A. Wahab. Mechanomyography and muscle function assessment: a review of current state and prospects. *Clin. Biomech.* 29:691–704, 2014.
[19]Karu, Z. Z., W. K. Durfee, and A. M. Barzilai. Reducing muscle fatigue in FES applications by stimulating with N-let pulse trains. *IEEE Trans. Biomed. Eng.* 42:809–817, 1995.
[20]Kirsch, N. A., X. Bao, N. A. Alibeji, B. E. Dicianno, and N. Sharma. Model-based dynamic control allocation in a hybrid neuroprosthesis. *IEEE Trans. Neural Syst. Rehabil. Eng.* 26:224–232, 2018.
[21]Knowlton, G. C., R. L. Bennett, and R. McClure. Electromyography of fatigue. *Arch. Phys. Med. Rehabil.* 32:648–652, 1951.
[22]Levenberg, K. A method for the solution of certain nonlinear problems in least squares. *Q. Appl. Math.* 2:164–168, 1944.
[23]Lubinski, M. A., S. Y. Emelianov, and M. O'Donnell. Speckle tracking methods for ultrasonic elasticity imaging using short-time correlation. *IEEE Trans. Ultrason. Ferroelectr. Freq. Control* 46:82–96, 1999.
[24]Marquardt, D. W. An algorithm for least-squares estimation of nonlinear parameters. *J. Soc. Ind. Appl. Math.* 11:431–441, 1963.
[25]Mizrahi, J. Fatigue in muscles activated by functional electrical stimulation. *Crit. Rev. Phys. Rehabil. Med.* 9:93–129, 1997.
[26]Moré, J. J. The Levenberg–Marquardt algorithm: Implementation and theory. In: Numerical Analysis, edited by G. A. Watson. Lecture Notes in Mathematics, Berlin: Springer, 1978. https://doi.org/10.1007/BFb0067700.
[27]Riener, R., J. Quintern, and G. Schmidt. Biomechanical model of the human knee evaluated by neuromuscular stimulation. *J. Biomech.* 29:1157–1167, 1996.
[28]Rogers, D. R., and D. T. MacIsaac. EMG-based muscle fatigue assessment during dynamic contractions using principal component analysis. *J. Electromyogr. Kinesiol.* 21:811–818, 2011.
[29]Sadoyama, T., and H. Miyano. Frequency analysis of surface EMG to evaluation of muscle fatigue. *Eur. J. Appl. Physiol. Occup. Physiol.* 47:239–246, 1981.
[30]Sayenko, D. G., R. Nguyen, M. R. Popovic, and K. Masani. Reducing muscle fatigue during transcutaneous neuromuscular electrical stimulation by spatially and sequentially distributing electrical stimulation sources. *Eur. J. Appl. Physiol.* 114:793–804, 2014.
[31]Sheffler, L. R., and J. Chae. Neuromuscular electrical stimulation in neurorehabilitation. *Muscle Nerve* 35:562–590, 2007.
[32]Sheng, Z., N. Sharma, and K. Kim. Quantitative assessment of changes in muscle contractility due to fatigue during NMES: an ultrasound imaging approach. *IEEE Trans. Biomed. Eng.* 2019. https://doi.org/10.1109/tbme.2019.2921754.
[33]Shi, J., Y. P. Zheng, X. Chen, and Q. H. Huang. Assessment of muscle fatigue using sonomyography: muscle thickness change detected from ultrasound images. *Med. Eng. Phys.* 29:472–479, 2007.
[34]Shinohara, M., and K. Søgaard. Mechanomyography for studying force fluctuations and muscle fatigue. *Exerc. Sport Sci. Rev.* 34:59–64, 2006.
[35]Siracusa, J., K. Charlot, A. Malgoyre, S. Conort, P.-E. Tardo-Dino, C. Bourrilhon, and S. Garcia-Vicencio. Resting muscle shear modulus measured with ultrasound shear-wave elastography as an alternative tool to assess muscle fatigue in humans. *Front. Physiol.* 10:626, 2019.
[36]Taelman, J., J. Vanderhaegen, M. Robijns, G. Naulaers, A. Spaepen, and S. Van Huffel. Estimation of muscle fatigue using surface electromyography and near-infrared spectroscopy. In: Oxygen Transport to Tissue XXXII. New York: Springer, 2011, pp. 353–359.
[37]To, C. S., R. Kobetic, J. R. Schnellenberger, M. L. Audu, and R. J. Triolo. Design of a variable constraint hip mechanism for a hybrid neuroprosthesis to restore gait after spinal cord injury. *IEEE/ASME Trans. Mechatronics* 13:197–205, 2008.
[38]Vøllestad, N. K. Measurement of human muscle fatigue. *J. Neurosci. Methods* 74:219–227, 1997.
[39]Winter, D. A. Biomechanics and Motor Control of Human Movement. Hoboken: Wiley, 2009.
[40]Witte, R. S., K. Kim, B. J. Martin, and M. O'Donnell. Effect of fatigue on muscle elasticity in the human forearm using ultrasound strain imaging, 2006. https://ieeexplore.ieee.org/iel5/4028925/4030573/04398449.pdf.
[41]Yoshitake, Y., H. Ue, M. Miyazaki, and T. Moritani. Assessment of lower-back muscle fatigue using electromyography, mechanomyography, and near-infrared spectroscopy. *Eur. J. Appl. Physiol.* 84:174–179, 2001.